2018

Mechanisms of stabilization of expansive soil with lignosulfonate admixture

Dennis Pere Alazigha
University of Wollongong, dpa902@uowmail.edu.au

Buddhima Indraratna
University of Wollongong, indra@uow.edu.au

J S. Vinod
University of Wollongong, vinod@uow.edu.au

Ana Heitor
University of Wollongong, aheitor@uow.edu.au

Mechanisms of stabilization of expansive soil with lignosulfonate admixture

Abstract

This study investigated and identified the mechanisms by which a remoulded expansive soil was modified or altered by a non-traditional admixture, lignosulfonate (LS). To achieve this objective, untreated and LS treated samples of expansive soil were examined microscopically using X-ray Diffraction (XRD), a Scanning Electron Microscope coupled with Energy Dispersive Spectroscopy (SEM/EDS), Fourier Transform Infrared (FTIR), Computed Tomography (CT-Scan), Nuclear Magnetic Resonance (NMR), Cation Exchange Capacity (CEC), and the role of Specific Surface Area (SSA). The interest was to identify and compare any physical and chemical changes between the untreated and treated samples and then propose the most likely reaction modes between the admixture and the soil minerals.

The results indicated that the percent swell is intimately related to the amount of water that is adsorbed by the expansive clay minerals. Furthermore, the amount of moisture in an expansive soil is influenced by a small addition of organic (cationic) compound such as LS. The adsorption of LS on the mineral surfaces provided waterproofing effect on soil due to the hydrophobic nature of LS, which in turn contributed to a decrease in the extent of swelling of the otherwise expansive soil. The basal and peripheral adsorption of LS led to smearing and subsequent agglomeration of soil particles restricting water ingress into the soil body. In addition, the cationic exchange between the admixture and the soil particle surfaces (i.e. replacing the negative surfaces on clay lattices) prompted flocculation, which further decreased the soil's affinity to water.

Disciplines

Engineering | Science and Technology Studies

Publication Details

Alazigha, D., Indraratna, B., Vinod, J. S. & Heitor, A. (2018). Mechanisms of stabilization of expansive soil with lignosulfonate admixture. Transportation Geotechnics, 14 81-92.

MECHANISMS OF STABILIZATION OF EXPANSIVE SOIL WITH LIGNOSULFONATE ADMIXTURE

Dennis Pere Alazigha[1], Buddhima Indraratna[2], Jayan S. Vinod[3], Ana Heitor[4]

Abstract

This study investigated and identified the mechanisms by which a remoulded expansive soil was modified or altered by a non-traditional admixture, lignosulfonate (LS). To achieve this objective, untreated and LS treated samples of expansive soil were examined microscopically using X-Ray Diffraction (XRD), a Scanning Electron Microscope coupled with Energy Dispersive Spectroscopy (SEM/EDS), Fourier Transform Infrared (FTIR), Computed Tomography (CT-Scan), Nuclear Magnetic Resonance (NMR), Cation Exchange Capacity (CEC), and the role of Specific Surface Area (SSA). The interest was to identify and compare any physical and chemical changes between the untreated and treated samples and then propose the most likely reaction modes between the admixture and the soil minerals.

The results indicated that the percent swell is intimately related to the amount of water that is adsorbed by the expansive clay minerals. Furthermore, the amount of moisture in an expansive soil is influenced by a small addition of organic (cationic) compound such as LS. The adsorption of LS on the mineral surfaces provided waterproofing effect on soil due to the hydrophobic nature of LS, which in turn contributed to a decrease in the extent of swelling of the otherwise expansive soil. The basal and peripheral adsorption of LS led to smearing and subsequent agglomeration of soil particles restricting water ingress into the soil body. In addition, the cationic exchange between the admixture and the soil particle surfaces (i.e. replacing the negative surfaces on clay lattices) prompted flocculation, which further decreased the soil's affinity to water.

Key words: Stabilization With Admixtures, Physical-Chemical Interactions of Soil and Rock, Geotechnics of Sustainable Construction

Nomenclature

LS	Lignosulfonate
XRD	x-ray diffractogram
SEM	scanning electron microscope
EDS	energy dispersive spectroscopy
FTIR	fourier transform infrared
^{1}H-NMR	hydrogen nuclear magnetic resonance
CT	computed tomograph
CEC	cation exchange capacity
SSA	specific surface area
D_2O	deuterated water
TMS	tetramethylsilan
δTMS	chemical shift
d001	001 interlayer spacing
2θ	refractive angle
-OH	hydroxyl
H-O-H	water molecule
MIR	mid infrared
NIR	near infrared
νOH	-OH stretching
2δOH	-OH bending
2νw	strong hydrogen bond
BET	Brunauer, Emmett and Teller
MB	methylene blue

[1]PhD candidate, Centre for Geomechanics and Railway Engineering, Univ. of Wollongong, Wollongong City, NSW 2522, Australia. E-mail: dpa902@uowmail.edu.au

[2] Distinguished Professor of Civil Engineering, Director, Centre for Geomechanics and Railway Engineering, Univ. of Wollongong, Wollongong City, NSW 2522, Australia. Email: indra@uow.edu.au

[3]Senior Lecturer, Centre for Geomechanics and Railway Engineering, Univ. of Wollongong, Wollongong City, NSW 2522, Australia E-mail: vinod@uow.edu.au

[4]Senior Lecturer, Centre for Geomechanics and Railway Engineering, Univ. of Wollongong, Wollongong City, NSW 2522, Australia E-mail: aheitor@uow.edu.au.

Words: 6963; **Figures**: 11; **Tables**: 2

Submitted to: Transportation Geotechnics

Author for correspondence: Dr Jayan S. Vinod,
University of Wollongong, Wollongong City, NSW 2522, Australia
Ph: +61 2 4221 4089, Fax: +61 2 4221 3238,
E-mail: vinod@uow.edu.au

Introduction

The effect of non-traditional admixtures (e.g. organic polymers) on the geotechnical properties of soils have been reported by various researchers (e.g. Rauch et al. 2003; Tingle et al. 2007; Athukorala et al. 2013; Chen and Indraratna, 2014, 2015; Chen et al. 2015). For example, Indraratna et al. (2008); Vinod et al. (2010); Chen et al. (2014), reported significant increase in strength of LS treated silt soils after 7 days of curing. However, the volume of literature available on the microstructural characterization of soils improved by these products, and in particular for expansive soil stabilized with lignosulfonate, is scarce. An understanding of the stabilizing mechanisms of non-traditional admixtures such as lignosulphonate (LS) is of vital importance if a wider acceptance is expected for this admixture. Given that LS is a waste by-product of paper and timber industry and is chemically established as a non-toxic compound (Indraratna et al. 2008; 2010), its use for soil stabilization has considerable merit in contrast to highly alkaline and sometimes corrosive chemical admixtures that are lime and cement based. In spite of the potential advantages offered by traditional admixtures in terms of shear strength (Indraratna et al 2008), their use for ground improvement has often been restricted by stringent environmental criteria, where adverse effects on groundwater and soil chemistry changes have been a major concern (Rauch et al. 2003).

The purpose of this study is to investigate and identify the mechanisms by which an expansive soil was altered by the LS admixture using analytical techniques such as X-Ray Diffraction (XRD), Scanning Electron Microscope (SEM), SEM coupled with Energy Dispersive Spectroscopy (SEM/EDS), Fourier Transform Infrared spectroscopy (FTIR), Nuclear Magnetic Resonance (NMR), X-Ray Computed Tomography (CT-Scan), Specific Surface Area (SSA), and as well as Cation Exchange Capacity (CEC) tests.

Expansive Soil Characteristics

The expansive soil was collected at Gunnedah, Queensland, Australia, at a depth of 250 – 700mm. The liquid limit (LL) and plasticity index (PI) of the soil were 91% and 51 respectively thus, it could be described as inorganic silty clay of high plasticity (CH). The mineralogy of the soil was determined quantitatively using siroquant analysis (Taylor 1991). The results showed that by mass, 36% was clay (i.e. 12.7% kaolinite, 10.4% montmorillonite, 4.4% illite and 8.5% montmorillonite-chlorite), while gibbsite, halite, rutile, hematite and quartz were 7.6%, 4.8%, 2.3%, 3.5%, 12.1% and 24.8%, respectively (Alazigha, 2015).

The soil was dried to constant mass, then crushed and sieved through a 1.18mm aperture sieve, and this material passing through was used to prepare the test specimens for LS treatment. The physical/chemical properties of the remoulded soil are presented in Table 1. Detailed analysis by Alazigha (2015) using energy dispersive spectroscopy has shown that this soil predominantly contains Si^{4+}, Al^{3+} and Mg^{2+} as octahedral cations and Na^{+}, Ti^{+}, K^{+}, and Ca^{2+} as exchangeable interlayer cations. In particular, the presence of Na^{+}, Ti^{+}, and K^{+} also support that the soil contains montmorillonite. According to Grim (1968), the valency of cations affects the thickness of diffuse double layer (DDL) in clays; i.e. the lower the valency of exchangeable cations (e.g. Na^{+}, Ti^{+}, and K^{+}) in the DDL of clay particles, the more susceptible are the clay particles to interparticle repulsion (swelling).

The one-dimensional oedometer free swell test (ASTM D4546) of the remoulded soil conducted under an initial seating load of 7kPa showed that the percent swell is approximately 6%. A 7-day curing period was chosen for all test specimens based on previous research works (Chen and Indraratna 2015; Indraratna et al. 2008; Vinod et al. 2010).

According to the classification scheme proposed by Seed et al. (1962), the soil can be classified as “high” expansive (i.e. percent swell = 5 - 25%). The soil shrinkage limit is 9% (Table 1) which is

also in agreement with the same class of expansiveness (7 – 12%). The soil activity (activity > 1.25) also supports the expansive nature of the tested soil (Skempton, 1953).

Characteristics of lignosulfonate

Lignosulfonate (LS) is a waste by-product of the paper manufacturing industry with an estimated global annual production of 50 million tons (Gandini and Belgacem 2008). Depending on the type of timber/paper industry, the LS may be extruded either as predominantly calcium, magnesium or aluminium based organic compound (benzene ring as the basic body). The industry is currently facing the challenge on the best possible means of its disposal. It is envisaged that with a well-documented scientific evidence of LS-based soil improvement mechanisms of stabilization, the application of this by-product will gain wider publicity and greater acceptance in sustainable infrastructure construction and slope stabilization projects.

The chemical structure (Table 1, 2 and Fig 1) of the LS was investigated using EDS, FTIR, and ^{1}H-NMR techniques, respectively. Based on the results obtained through these tests, a chemical structure of the proprietary chemical has been proposed by Alazigha et al. (2016). It can be observed that this LS compound (Fig 2) is a highly cross-linked amorphous polymer consisting of aliphatic (i.e. negative - hydrophilic sulphite, hydroxyl, methoxyl, carboxyl, phenolic groups) and aromatic (i.e. positive - hydrophobic aromatic structure) portions, but its net potential is negative. Its basic chemical structure showing a benzene ring is capable of forming complexes with cations such as Ca, Na and Mg, enabling it to compete for adsorption sites in clays or could form covalent coordinate bonds with multivalent metal ions. The chemical structure shows a coordinating polyvalent calcium cation (Ca^{2+}), thus the LS used in this study could be classified as a calcium lignosulfonate.

Specimen preparation and methods of micro-characterization

The micro-characterization study and subsequent identification of stabilization mechanisms of LS on expansive soil was achieved through a number of instrumental analytical techniques. The physical/chemical changes with and without LS addition were evaluated and compared to provide an insight into the possible reaction mechanisms. The percent swell of the remoulded soil with and without LS treatment were assessed in accordance with the procedure suggested in ASTM (D4546). The main objective was to determine whether the addition of LS translated into beneficial change in swelling behaviour of the compacted expansive soil at optimum moisture content = 38%, and maximum dry unit weight = 13.1kN/m3). At least three identical specimens were prepared for checking test repeatability.

An X-ray diffractometer (GBS Scientific Equipment) was used to perform scans for untreated and LS treated soil specimens with the following generator settings: input voltage 35.0kV, current 28.5mA and CuK radiation. Other parameters included wavelength (λ) = 1.54056Å, angle scan (2): 2° - 60° using a 0.02° step size and dwelling time (speed) of 10/min at each step. To minimise the influence of temperature and humidity variations during the measurement, the tests were carried out in the laboratory with 98% relative humidity and at a constant temperature of 18oC. Oriented specimens were prepared on glass slide as suggested by Whittig and Allardice (1986). In addition, X-ray CT-scan technique was employed to probe non-destructively the microstructure of the compacted specimens before and after the one dimensional swell test. A Toshiba Asteion S4 X-ray CT scanner was used with the following settings: the X-ray tube voltage was 135kV, current was 200mA, X-ray beam (slice thickness) was 3mm wide, exposure time was 1s, and the field of view (FOV) was 21cm with a zooming factor of four. The acquired images were processed using medical radiology software DicomWorks v. 1.3.5 (Puech et al., 2007). This included adopting adequate window ranges and post-processing filtering techniques.

For the SEM analysis, additional compacted specimens prepared for swell test and cured for 7 days were carefully broken down to smaller size (approximately 1mm) and then placed on a 20mm diameter SEM sample holder exposing the "fresh" surface. The untreated and 2%LS treated specimens were then inserted into a JEOL JSM-840A SEM at 20kV, equipped with EDS to study morphological variations. For the quantitative identification of elemental composition in soil with and without treatment, the EDS component was used.

FTIR was also used in this study to identify the chemical bonds formed, by measuring the frequencies at which absorption of the infrared radiations occurred. FTIR was performed using a Shimadzu IRAffinity-1 C 8984 Model instrument at characteristic wavenumbers of 7000 and 400cm^{-1}. For each sample, 120 scans were recorded with a resolution of 4cm^{-1}. Possible function groups in LS were further probed using aromatic protons nuclear magnetic resonance (^{1}H-NMR) spectroscopy. The spectrum was recorded using a Varian Gemini 300-Hz apparatus using a sweep width of 4000Hz, a pulse width of 7.2ms, and a temperature of 297K. Deuterated water (D_2O) and tetramethylsilan [TMS; (CH3)4Si] were used as internal standard whose chemical shift (δTMS) was taken as zero (0.00ppm).

Finally, the roles of cation exchange capacity (CEC) and the specific surface area (SSA) were investigated to evaluate the effect of the addition of the admixture on these properties (ASTM C 837).

Results and discussion

Effect of LS on the swell behaviour of the remoulded expansive soil

The swell behaviour of the remoulded expansive soil was determined through a standard one dimensional swell test (ASTM D4546). Untreated and LS treated soil specimens were tested, and the results indicate that LS has a substantial effect on the magnitude and rate of the percent swell with time (Fig. 3). The percent swell decreased with increasing LS content. However, the percent swell of the soil decreased maximally from 6% to about 4.6% with 2% LS addition. The decrease in the swell magnitude is related to the decrease in the amount of adsorbed moisture in treated soil specimen. This is corroborated by the moisture content determination at the end of the swell test. For the untreated, 0.5%, 1.0%, 2.0%, and 3.0% treated specimens, moisture content of 51.0%, 49.7%, 48.6%, 47.0%, and 47.8% was measured, respectively. This indicates that the addition of LS may have inhibited the absorption of water, thus resulting in the decreased percent swell and as well as a lower swelling rate (Fig 3). However, For the 2% and 3% LS treated specimens, a slight increase in percent swell with time (after 20000hrs) was observed. As LS behaves like an expanding polyelectrolyte because it carries a strong negative charge which is counter-balanced by positively charged cations dispersed in the diffuse double layer of clay. So, at about or beyond optimum content of LS, the excess molecules of LS which did not participate in the stabilization process in treated soils due to spent cations in clay result in mutually repulsive forces between the charged sections of the LS chain, causing the molecules to expand. This is possibly why the slight increase in percent swell for 2% LS treated specimens after 20000hrs. For the same reason, the 3% LS treated specimen exhibited higher percent swell than 2% treated specimen.

Microstructural characterization of admixture mechanisms

XRD analysis:

XRD was used to determine the arrangement and spacing of atoms within soil crystals, to qualitatively identify clay minerals in the soil and to assess changes in clay mineralogy associated with the addition of 2% of LS. The diffractograms of the untreated (LS=0%) and treated (LS=2%) specimens are shown in Fig. 4. It was observed that both samples contained smectite, illite, kaolinite, quartz groups, and layers of mixed minerals.

Changes in the refractive angle (2θ) which translate to changes in the d-spacing in soil minerals were determined by evaluating the d_001 smectite peak at 2θ = 5.780 in the specimens with and without treatment. There is a noticeable change in the d_001 peak that resulted from the addition of LS, such that the peak area becomes smaller i.e. less d_001 surface area. The decreased peak surface area is attributed to a decrease in the average size of crystallite in the reflecting minerals. According to Cullity (1979), large crystallites exhibit sharp peaks but as they decrease in size, so do the width of the peak and that amorphous samples display hump shaped peaks. This indicates that the changes in the shape observed for the d_001 smectite peak, resulting by the addition of LS may have been induced by the amorphocity of the LS admixture. This in turn suggests that, LS addition plays a significant role in the crystallographic alteration of the d_001 smectite minerals observed in the treated specimens. Further, the basal and peripheral coating of the smectite minerals by the LS admixture, a non-crystalline polymer, likely restricted diffraction from the characteristic atomic planes of the clay minerals thus, the d_001 smectite peak broadened after treatment.

The d_001 smectite peak also shifted to the left on the 2θ axis upon treatment. The shift in this peak from $2\theta = 5.78^0$ to 5.38^0 for untreated and treated specimens, respectively, caused a corresponding initial increase in the d-spacing of the smectite minerals from 13.90 to 14.93Å

(Bragg's law). This was due to the crystalline domains of the mineral lattices relaxing as the ion-carrier and cross-linking agent (LS) intruded the inner layer, leading to initial expansion of the inner layer and subsequent moisture entrapment. These findings suggest that for soil treated with 2% LS, the admixture intercalated the layers of expansive clay minerals that caused their initial expansion. This result is consistent with the mechanism of interlayer expansion with subsequent moisture entrapment proposed earlier by Scholen (1991; 1995) and Rauch et al. (2003) for non-standard chemical stabilizers (e.g. polymers, enzymes, electrolytes, sulfonated limonene).

It is important to note the peaks of non-swelling soil minerals such as kaolinite and quartz that did not shift along the 2θ axis in the specimen treated with LS. While the d-spacing of these minerals in the specimens with and without treatment was practically the same, their associated intensities decreased significantly. This could be indicative of the inability of LS admixture to intercalate the inner layers of non-expansive soil minerals, which results in peripheral adsorption alone causing a decrease in the intensities of the minerals. The reduction in intensity in the diffractograms of the minerals is ascribed to a decrease in the concentration of the particular minerals. This indicates that the external adsorption of LS on these minerals likely reduced the availability of the mineral crystals to reflect incident rays, resulting in a decrease in the peak intensities hence, the less-availability of the minerals to adsorb water molecules.

Scanning Electron Microscope (SEM) analysis

The morphological changes upon the addition of 2% LS were investigated using a JEOL JSM-6460LA SEM, equipped with a Minicup EDS. The SEM micrographs of the untreated specimens, taken at a magnification factor of x2500 (Fig 5a), reveal that the fabric consists mainly of dense clay matrices with little or no appearance of aggregations. A poorly open and/turbulent type of microstructure, with smectite lamelle in a fairly orderly arrangement can be observed towards the centre of the micrograph. The minimal appearance of the 'cornflake' like clay minerals usually

associated with the smectite group could be attributed to the structural breakdown due to remoulding of the soil.

In contrast, the SEM micrographs of the LS treated specimens indicate that the morphology of the soil changed considerably upon addition of LS. Fig 5b shows the presence of flocculated particles with sharper edges. These morphological changes can be attributed to the adsorption/coating mechanisms and cation exchange processes between the soil minerals and the LS complex. Fig 5b also shows that the clusters of clay particles were interspaced by larger but fewer pore spaces compared to those of the sample of untreated soil. This suggests that the sample treated with 2% LS, flocculated more than the untreated counterpart, and that the ingress of water into the entire soil body would have been restricted, resulting in a decrease in the magnitude of swell potential as mentioned earlier (Fig 3).

Energy dispersive spectroscopy (EDS) analysis

The EDS spectrum for the untreated and LS treated specimens are presented in Figs 6a and b. It can be observed that there was practically no difference in intensity in the EDS spectra of the specimens. This suggests that no new element(s) were formed between the sorbent (soil minerals) and the sorbate (LS admixture) complex, although the treated sample shows small traces of sulphur (S) and an increase in the carbon (C) content, possibly due to the presence of an unreactive carbon and sulphite group in the organic chemical structure of the LS admixture (Fig. 2).

In terms of quantitative elemental composition in each specimen, the change in the ratio of elements following LS treatment was insignificant; for example, the ratio of Al:Si varied by about 8.1%. These two elements (Al and Si) were chosen because they form the basic units of clay minerals so if there was a significant decrease in the aluminium-silica ratio after treatment, this would have indicated a form of chemical alteration. In contrast, if the Al:Si ratio had increased

then silica may have been released from the clay minerals. The amounts of aluminium and silica in the untreated soil were 15.34g and 48.85g, respectively, and 14.21g and 41.61g, respectively for the soil with LS treatment. The amount of aluminium and silica were almost the same, but the Al:Si ratio increased slightly from 0.3140 to 0.3415 after treatment; suggesting negligible chemical reactions. The results from EDS corroborated well with those from XRD data which showed that the LS treatment functioned through crystallographic alteration of the mineral lattices.

While the data obtained from Al:Si analysis can be used to corroborate the XRD findings, due caution must be exercised as EDS results could be affected by the topography of the specimen. To minimise the effect of the specimen topography on the test data, all the specimens were prepared identically. Moreover, multiple samples (five) were analysed in each case and averaged to quantitatively determine their elemental compositions.

X-ray CT-scan:

In recent years, X-ray CT scan techniques have been employed to describe physically complex pore spaces with respect to variables such as the bulk density of soil (e.g. Anderson et al. 1990; Heitor et al. 2013). Fig 7 shows a typical CT-scan image of a test specimen that was examined using this technique. Figures 7a and c show the CT scan images of the untreated compacted specimens before and after one-dimensional swell tests, while Figs. 7b and 7d denote 2% LS treated specimens before and after one-dimensional swell tests, respectively.

Each pair of images was processed to reflect the same grayscale window centre and width (Puech et al. 2007) to allow for a qualitative comparison between the partially saturated and fully saturated specimens. Typically, the comparative density of the materials can be identified by a difference in colour from the greyscale, e.g. white/light grey represents the water phase whereas black denotes the air phase, and darker grey is the solid phase (Fig 7). However, due to limitations

in the scanner's resolution (1mm), the structural changes in the soil were only evaluated in terms of macroscopic pores; i.e. the lighter colour shades symbolise high macroscopic water saturation, while the darker areas represent less saturated phases. It can be easily observed that variations in the moisture content of samples occurred for the untreated and treated specimens, but the geometry of the pore space structure could not be detected. It was very clear that, the degree to which the specimen of expansive soil was saturated was undoubtedly affected by the LS admixture (Figs. 7c and 7d). Close examination of both images after the swell test reveal a more prominent darker area (existence of air phase) in the treated specimen compared to the untreated specimen. Presumably, the presence of LS limited the adsorption of moisture by soil minerals into the macro-pores of the treated sample. The hydrophobic component of LS may have hindered the ingress of moisture into the pore spaces, and the intercalation of the admixture into the inner layers of the expansive minerals might have displaced water molecules from the soil body. This observation is in agreement with the water content determinations conducted at the end of the swell test which showed a decrease of 7.8% in moisture for the LS treated specimen, as stated earlier.

Fourier Transform Infrared spectroscopy (FTIR)

Spectrum of untreated soil

The FTIR technique was used to investigate the vibrational behaviour of the –OH, H-O-H, interlayer cations, tetrahedral silicate/aluminate anions, octahedral metal cations and as well as identify the soil mineralogy. The infrared spectra for each sample was recorded with 120 scans in the near-infrared (NIR) and mid-infrared (MIR) spectral regions in a transmission mode at $4cm^{-1}$ resolution.

Past research studies reported that the absorption bands at the near-infrared (NIR) region of 6800-$7000cm^{-1}$ are the signature vibrations of water molecules as shown in Fig 8a. Bands at 6984, 6976,

6872, 6802, 6740, and 5570cm^{-1} is -OH vibration modes of water (Bishop et al. 1994). Petit et al. (1999) reported that the –OH stretching (νOH) and binding (2δOH) combination (νOH + 2δOH) modes associated with inner-surface and inner hydroxyl groups were synonymous with bands at 5484cm^{-1} and at 5040-5420cm^{-1}, respectively in Fig 8b. The peaks at 6976 and 5250cm^{-1} correspond to -OH bending overtone of FeFeOH and combinations involving inner sphere and surface H_2O molecules, respectively. Combinations of –OH stretching bands of kaolinite with lattice deformation vibrations were seen between 4300- 4000cm^{-1} in Fig 8b.

The pattern also showed common bands for all dioctahedral smectite. For example, the shoulder at 6852cm^{-1} was assigned to H-O-H molecules involved in strong hydrogen bonds (2νω). The strong bands at 5253 and 5342cm^{-1} were caused by smectite minerals due to a combination of the stretching (νOH) and bending (δ) vibrations of water and (νOH + δAlFeOH) combination modes, respectively (Komadel 1999). The band at 4520cm^{-1} is attributed to a combination of -OH stretching linked to AlAlOH group, while the 4624cm^{-1} band is the deformation vibrations of AlAlOH groups.

In the Mid Infrared region (400 – 4000cm^{-1}; Fig. 9a, b, & c), the broad band at about 3000 – 3800cm^{-1} (Fig. 9a) is exclusively associated to sorbed H-O-H with the – OH stretching vibration peak of water centred at 3365cm^{-1}. The shoulder at 3393cm^{-1} was assigned to –OH stretching of structural hydroxyl groups in smectite. The 3620cm^{-1} characteristic band is inner -OH and the 3645-3697cm^{-1} bands are the vibrations of the external –OH. The band at 3593cm^{-1} was assigned to the –OH stretching mode of kaolinite group. The symmetrical and anti-symmetrical stretch of C-H mode of $–CH_2$ group are associated with the bands at 2993cm^{-1} and 2900cm^{-1} (Fig 9a), respectively while the band at about 2868cm^{-1} was attributed to symmetric stretch of $–CH_3$ group of kaolinite (Russell and Fraser 1996; Saikia and Parthasarathy 2010).

In Fig. 9b, the bands at 2300 and 2364cm^{-1} were assigned to CO_2 derived from the environment. The significant infrared band observed at 1620 – 1740cm^{-1} is assigned to water HOH bending mode. This suggests that there is water present in the montorillonite structure. The band at 1640cm^{-1} corresponds to strongly bonded water, whereas the band at 1635cm^{-1} is attributed to less strongly bonded water and corresponds to the position of the water bending mode of liquid water. The multiple bands at 1364-1620cm^{-1} were associated with C-H, Na^+ and SiO_4 vibrations. (Bishop et al. 1994; Komadel et al. 1999).

Bishop et al. (1994) assigned 1116cm^{-1} band to the –OH vibrational mode of the hydroxyl molecule in smectite. In Fig 9c, the bands at 510 and 464cm^{-1} were due to Si-O-Al (where Al is an octahedral cation), Al-OH groups, or Si-O-Si bending vibrations, respectively. The band at 776cm^{-1} and the weak shoulder at 785cm^{-1} represent quartz mineral in the soil, and this was confirmed by X-Ray data. The absorption bands at 918, 879cm^{-1} and 827cm^{-1} in clay is -OH bending vibrations of AlFeOH, (Al2OH) and AlMgOH minerals in smectite, respectively. The -OH bending vibrations at these wave numbers suggested that the Al octahedral was partially substituted by Fe and Mg. The 1003cm^{-1} band is a fingerprint vibration –OH deformation of gibbsite.

Spectrum of soil treated with 2% LS:

The NIR of 4000-7000cm^{-1} of the sorbent-sorbate complex (Fig 8a & b) showed insignificant spectral differences to the sorbent spectrum, probably because the adsorbed LS molecules did not adopt a regularly organized structure at the soil mineral surfaces. However, identifiable band shifts/deformations were seen after 2% LS was added. For example, the near disappearance of the bands at 6972, 6872, 6740, and 6802cm^{-1} was associated with a decrease in the amount of interlayer water. The bands (5040-5420cm^{-1}) assigned to a combination of stretching and bending vibrations of water decreased in intensity after the addition of LS, which suggested there was

dehydration in the already collapsed inner layers of the expansive mineral lattices. These findings are in agreement with those of Bishop et al. (1994).

Moreover, the spectrum of the 2% LS treated soil at 6905 and 5342cm^{-1} show that the transmittance became sharper and more symmetrical, which indicated dehydrated conditions. Under dehydrated conditions the interlayer water was bounded to cations or interlayer surface which caused the H-O-H stretching vibration bands to shift to lower wavelengths than similar absorptions under hydrated conditions. This was clearly seen in the bands associated with HO-H vibrations at 6976, 6802, 6739, 6588, 6401, 6197, and 5815cm^{-1} in this investigation. Furthermore, the intensities of the bands at 5219 and 6802, 6621, 6467, 6303-6257, and 6104cm^{-1} increased after the addition of LS. This pattern in ionic treated soils is attributed to water directly coordinated to the cations forming hydrogen bonds with surrounding H2O molecules rather than the silicate lattice of the soil which is in agreement with Farmer and Russell (1971) and Theng (2012) observations and interpretations.

The transmittance intensity of the shoulder bands corresponding to inter-lamellar water (3200–400cm^{-1} and 1640cm^{-1}) indicates that most of its water was lost after the addition of LS, probably due to the displacement of water molecules as a consequence of the sorbate intercalation of the inter-lamellar space in the lattices of the expansive soil minerals. These perturbed water absorption bands shifted from 1640 to 1636cm^{-1} and 3365cm^{-1} to 3353cm^{-1}, which also suggests that the addition of LS leads to a decrease in the inner layer water content. The reduction in intensities and shifts associated with the above peaks suggested that LS underwent basal and peripheral adsorption on soil particles. This reduction in band intensities could also indicate that the water molecules remaining at the inter-lamellar space were coordinated to LS molecules through a “water bridging” mechanism. It is also likely that some of LS molecules displaced water to become directly coordinated with the cation, as a consequence of the high polarizing strength of

the Ca^{2+} cation. This behavioural observation is similar to that of benzonitrile-montmorillonite and nitrobenzene-montmorillonite complexes reported by Theng (2012).

Furthermore, the -OH stretching vibration shifts to a lower frequency when the hydrogen bonding interactions become stronger. The -OH vibration bands at 3792-3930, 3365, 508, and 417cm^{-1} weakened considerably and/or shifted to lower wave numbers upon LS addition (Fig. 9a, b, & c). Such behaviour of peaks could be ascribed to a reduction in the interlayer water in the soil samples. This indicates that LS formed direct bonds with adsorbed cations or coordinate directly with adsorbed moisture. Further spectra analysis within the MIR region (400 – 4000cm^{-1}) after chemical modification of the soil caused an increase in peak intensity at 1020cm^{-1}, which could then be correlated with the undissociated sulfonic acid group in the LS admixture in treated soil. Similarly, the appearance of a subtle band at 2841cm^{-1} (Fig. 9a) assigned to C-H stretching suggested the presence of unreacted LS molecules in treated soil. The presence of sulphur molecules were also observed in the EDS spectrum of treated samples, which supports the FTIR data. The addition of 2% LS admixture produced higher intensity of -OH band at approximately 3597 - 3630cm^{-1} (Fig. 9a). Adsorption in this region is attributed to -OH molecules being strongly co-ordinated to Al^{3+} in the octahedral layer.

The sample of LS modified soil also showed higher band intensity at 1105cm^{-1} and a new peak at 467cm^{-1}. These bands suggested the formation of Si-O stretching vibrations for amorphous silica and implied that amorphous LS attacked silica mineral and deposited its footprint of amorphocity. The intensity of the -OH bending vibrations at 879cm^{-1} of AlFeOH decreased slightly after the admixture was added, indicating an alteration of the crystalline lattices of these minerals. This decrease in intensities depicted a quantitative reduction of AlFeOH. An important consequence of replacing inorganic with organic cations is that the surface of the clay becomes hydrophobic, which further supports the reduction in the affinity for water by treated soil minerals already noted

earlier by a decrease in the band intensity, and hence a reduction in the swell potential of an otherwise expansive soil.

Cation exchange capacity (CEC)

The methylene blue (MB) test is one of the most accurate and simplest methods to determine the CEC of soils, and it relies on the basis that clay minerals have a large surface area with negative charges that could be exchanged with methylene blue cations (Santamarina et al. 2002). Aqueous methylene blue (MB) is a cationic dye ($C16H18N3ClS^{+}$) with a corresponding molecular weight (MW) of 319.85g/mol that can be adsorbed onto negatively charged clay surfaces. The "spot-test" method of the methylene blue dye test was used to estimate the CEC of untreated and 2% LS treated expansive soil.

The "Spot-Test" method was carried out in accordance with ASTM C837. Typically, a solution of MB (1mL = 0.01meq) was prepared, and the test is carried out by adding 2.0g dry soil to 300mL of distilled water and stirring until a homogenous mixture is obtained. The pH of the soil-LS solution is then reduced to the 2.5 – 3.8 range by adding appropriate drops of sulphuric acid (0.1N) while stirring continuously. While the soil-water-acid solution was still on the mixer, 5mL of the MB solution was added in increments. After each addition of the MB solution, a drop of the soil-water-acid-MB complex was taken with a glass pipette and placed on a Whatman No. 1 filter paper disk to observe the appearance of the blue halo around the drop deposit in the filter paper. This procedure was repeated until the end point was reached which was indicated by the formation of a light blue halo around the drop (Fig 10).

The amount of adsorbed MB, quantifiable by the methylene blue index (MBI), provides an estimate of the CEC for each soil sample as follows (ASTM C837):

$$MBI = 0.5V \qquad (1)$$

Where

V = millilitres of MB solution required to reach the end point.

For the untreated soil sample MBI (CEC) was 57.5meq/100g whereas for the sample treated with 2% of LS the MBI (CEC) was 47.5meq/100g.

The results indicate that the LS admixture had little effect on the CEC of the remoulded expansive soil. The untreated soil had a CEC of 57.5meq/100g but this decreased to 47.5meq/100g upon 2% LS addition, which represents only 17% of the total ion exchange capacity. This is likely associated with the large molecular size (201,300.00g/mol; Fredheim et al. 2002) of LS polymer, which may have resulted in a "cover-up-effect" leading to an incomplete cation exchange mechanism between the soil minerals and the admixture. LS with coordinating polyvalent cations are tightly bonded to the polymer matrix through coordination and/or chelation, involving sulphonic and hydroxyl groups and these cations are not easily dissociated in an aqueous medium. This non-dissociation of polyvalent cations from LS structure is believed to have aided the aforementioned "cover-up-effect". This is consistent with the observations by Theng (2012). The LS used in this investigation had a coordinating polyvalent cation (Ca^{2+}). As Ca^{2+} tends to exchange monovalent cations (e.g. Li^{+}, Na^{+}), or Mg^{2+} ions on soil mineral surfaces, the LS structure accompanies the exchange process and tends to cover-up exchangeable sites leading to an incomplete cation exchange mechanism.

The determination of the CEC of a soil using the MB technique is an easy and quick method compared to the Standard Determination of CEC with Ammonium Acetate (Chapman, 1965). However, the current MB test ("spot-test") technique contains operator errors such as the ability to judge the test's end point.

Specific surface area (SSA):

The quantity of adsorbed MB enabled the SSA of the soil specimens to be estimated. The SSA of the untreated and 2% LS treated specimens were calculated using equation (2) proposed by Hang and Brindley (1970). From the maximum amounts of adsorbed MB, and by assuming that the area covered by one molecule of MB equals 130Å, which corresponds to the molecules lying flat on the clay mineral surfaces (Santamarina et al. 2002):

$$SSA = MBI = A_{MB} \times 0.01 \qquad (2)$$

Where

MBI = methylene blue index for the clay in meq/100g clay (an estimate of soil CEC), AMB = surface area of methylene blue molecule (130Å; 1Å = 0.1nm), 0.01 = normality of MB i.e. the concentration of the MB solution used.

Therefore, the SSA of the untreated soil sample was given as SSA = 74.75m^2/g and the SSA of the 2% LS treated soil sample was given as SSA = 61.75m^2/g.

The calculated SSA values of untreated and 2% LS treated samples were 74.75m^2/g and 61.75m^2/g, respectively. This suggests that LS admixture caused the soil particles to agglomerate by 17% through the cation exchange mechanism. Assuming that the difference between the two SSA values of samples (74.75-61.75m^2/g = 13.0m^2/g) represented the area of MB dye in actual contact with the soil minerals, as suggested by Ramachandran et al. (1962), 13.0m^2/g suggests that the actual contact area of Ca^{2+} with the soil minerals which governs the cation exchange mechanism was probably very small. This might likely be the reason for the "cover-up-effect" mentioned earlier. The SSA data also supports the XRD findings that showed no significant chemical reactions occurred in the LS stabilization mechanisms of expansive soil. However, the crystallography of soil mineral was altered mainly through chemo-adsorption (hydrogen bonding),

and/or ionic bonding of LS molecules to form direct bonds with cations and hydroxyl groups on soil mineral surfaces and a minimal cation exchange mechanism.

In this investigation, the methylene blue (MB) test method was the preferred method for SSA determination. While commonly the SSA is determined using nitrogen (N_2) BET analysis technique, this method enables only the measurement of the external surface area of particles due to the inability of N_2 molecules to intercalate the inner layer of dry expansive soil lattices. For this reason, SSA values determined using the BET method are usually smaller (Ramachandran et al. 1962). Another traditional method of measuring SSA is the Ethylene Glycol Monoethyl Ether (EGME) technique. Though this technique measure the total surface area (internal and external), it is limited to a single partial pressure (P/Po) equilibrium, samples cannot be used multiple times, and it is time intensive (Cerato and Lutenegger, 2002). In contrast, the MB test was conducted on a soil-water suspension where the inner-layers of the weakly bonded silica sheets of smectite are easily intercalated by water or MB ions, which enable the internal and external surface layers to be measured. The corresponding areas determined by the N_2 BET adsorption method for the same samples were 62.45m^2/g and 49.85m^2/g for untreated and 2% LS treatment, respectively.

Proposed stabilization mechanisms of expansive soil treated with LS

The micro-characterization study and subsequent identification of the stabilization mechanisms of LS treated expansive soil was achieved through a number of instrumental analytical techniques. The physico-chemical changes before and after LS addition was evaluated and compared to provide insights into possible stabilizing mechanisms of the admixture on the expansive soil.

The findings suggested that the primary stabilizing mechanisms of LS admixture is via adsorption onto the surfaces of soil minerals through electrostatic interactions, hydrogen bonding, covalent bonding, and as well as cation exchange mechanisms with subsequent smearing, and agglomeration of soil particles (Fig 11). When LS is added to a remoulded expansive soil, it

intercalates the inner layer of expandable clay minerals and is adsorbed through mechanisms such as water bridging, hydrogen bonding, covalent bonding, and cation exchange mechanisms. However, EDS analysis showed that for non-expandable minerals such as quartz, the adsorption of LS was limited to the surface alone, probably due to the relatively larger molecular size of the polymer compared to the tightly held basal spaces of these minerals. The mechanism of adsorption of LS by soil minerals as the principle stabilizing mechanism is fully supported by data obtained from the analytical techniques (e.g. XRD, FTIR). For instance, the appearance of a new peak at 470cm^{-1} in the XRD results suggested that amorphous LS attacked the silica minerals and deposited its footprint of amorphicity.

The intercalation of LS into the lattices of the expansive minerals displaced water at the outer spheres of coordinating monovalent and divalent cations, where they then formed direct hydrogen bonds with the coordinated water or else developed covalent bonds in adsorbed cations in the soil. The intercalation of LS and subsequent adsorption on inner surfaces was accompanied by an initial expansion of the clay mineral lattices with subsequent moisture entrapment, as observed from the XRD micrographs. The adsorption of LS by soil minerals through hydrogen bonding led to the encapsulation of soil minerals with subsequent flocculation-agglomeration of the soil particles, as also observed in the SEM micrographs and reduced specific surface area of soil samples measured using the MB test.

Presumably, other mechanism corresponding to the ability of the cationic end of the admixture replacing the negative surface of the charged soil particles would have also contributed to particle flocculation and a decrease in the soil's affinity for water but to a smaller extent. The thin coating of soil particles by the organic cationic compound exposed its hydrophobic end (Fig 11) contributed to a reduction of the swell magnitude.

In summary, the stabilization mechanisms consist of the basal, and peripheral adsorption onto soil minerals through hydrogen bonding (water bridging), initial inner layer expansion with moisture entrapment, and covalent bonding (directly bonding to adsorbed cations) leading to the soil particles being coated, and with a subsequent reduction in the soil's affinity for water. The exchange of interlayer cations was also observed although is likely not significant due to "cover-up-effect".

The absence of significant new peaks (minerals) after treatment coupled with the negligible change in the soil mineral ratios (e.g. Al:Si) as obtained from EDS analysis of samples, suggested mainly inter-molecular interactions between soil minerals and the LS admixture rather than major chemical reactions. These mechanisms of the non-standard admixture collaborate well with the observations and interpretations of Scholen (1992; 1995).

Limitations of this study

The stabilizing mechanisms of LS reported above are based solely on tests conducted on a highly plastic (remoulded) expansive soil. This type of soil exists over hundred kilometres affecting transport corridors and was of keen interest to Roads and Traffic Authorities in Queensland and NSW, Australia. Therefore, while the established mechanisms are applicable for similar soil types, the nature of the data measured will inevitably vary from one soil to another, and depending in the montmorillonite content in each soil. Therefore, these results cannot be extrapolated directly to any other soil without exercising caution and prior laboratory testing to determine the efficiency of treatment as each soil reacts differently to the same LS and amount of chemical used.

Conclusion

Through a series of micro-characterization tests, the mechanisms by which LS, a non-traditional waste by-product, stabilized a remoulded expansive silty clay (highly plastic) were identified. The chemical admixture and the expansive soil were first characterized individually to establish their reactive products/baseline properties. The physical/chemical properties of the soil following LS treatment were then compared with untreated samples to determine whether the admixture prompted any changes. The impact of the addition of LS in the remoulded soil was found to be greater for the expansive clay minerals (e.g. montmorilonite) and less on the non-expanding clay minerals (e.g. kaolinite) and relatively inert, quartz.

On addition of LS, the organic molecules wedged into the structural sheets of the expansive clay minerals, displaced water and caused an initial increase in d-spacing which was demonstrated by x-ray diffraction. The FTIR analysis showed that intercalated admixture was then adsorbed through hydrogen bonding (water bridges), and/or bonded directly with the dehydrated cations. Moreover, this investigation also revealed that the admixture experienced cation exchange between Ca2+ in the admixture and soil cations (Na^{+}, Ti^{+}, Mg^{2+}) and contributed to particle flocculation confirmed by SEM micrographs. These mechanisms resulted in a ‘waterproofing effect’ on soil sample hence, the decrease in percent swell of treated expansive soil which was also confirmed by the X-ray, CT-scan micrographs and lower moisture contents measured for the specimen treated with LS.

For non-expanding clay minerals, only surface adsorption was observed and based on XRD data, significant chemical changes in clay mineralogy were not apparent, but changes in the crystalline nature of the adsorbent due to basal and peripheral adsorption of LS. This observation was supported by the minimal change in the Al:Si ratio, which was expected if the interaction of an admixture and soil was more by physical rather than chemical means. SEM studies visualized the

formation of LS films on the soil surface whereas the FTIR studies indicated participation by the surface sites of the sorbent in the adsorption mechanisms.

Acknowledgement

The authors wish to provide recognition to the Niger Delta Development Commission (Nigeria), the Australian Research Council (ARC) for the financial support. The authors are also grateful to Scott Morrison (Coffey Geotechnics) and Bob Amstrong (ChemSTAB). Thanks to Dr Qingsheng Chen and Dr Linda Tie for their valued suggestions. We also recognize Roza Dimeska, of the School of Chemistry, for guiding us in the use of the FTIR equipment. Finally, we acknowledge the Australian Research Council (ARC) for establishing the Electron Microscopy Centre (EMC) and Institute of Superconducting & Electronic Materials (ISEM) located at the University of Wollongong.

References

Alazigha, D.P., Indraratna, B., Vinod, J.S., and Ezeajugh, L.E. The swelling behaviour of lignosulfonate – treated expansive soil. Proceedings of the Institution of Civil Engineers, Ground Improvement, 2016; 169(13): 182-193.

Alazigha, D.P. The Efficacy of Lignosulfonate in Controlling the Swell Potential of Expansive Soil and its Stabilization Mechanisms. PhD thesis, University of Wollongong, New South Wales, Australia; 2015.

Anderson, S.H., Peyton, R.L., and Gantzer, C.J., Evaluation of constructed and natural soil macropores using x-ray computed tomography, Transport of water and solutes in macropores". Geoderma, 1990;46: 13–29.

ASTM D4546. Standard test Method for One-Dimensional Swell or Collapse of Cohesive Soils, West Conshoshocken, PA, USA;2008.

ASTM C837. Standard Test Method for Methylene Blue Index of Clay, West Conshoshocken, PA, USA; 2014.

Athukorala, R, Indraratna, B., and Vinod, J.S. Modeling the internal erosion behavior of lignosulfonate treated soil. In C. L. Meehan, D. Pradel, M. A. Pando & J. F. Labuz (Eds.), Geo-Congress 2013 (1872-1881). United States: American Society of Civil Engineers.

Bishop, J.L., Pieters, C.M., and Edwards, J.O. Infrared spectroscopic analyses on the nature of water in montmorillonite. Clays and Clay Minerals, 1994; 42: 701-715.

Cerato, A.B, Lutenegger, A.J. Determination of surface area of fine-grained soils by the ethylene glycol mono-ethyl ether (EGME) method. Geotechnical Testing Journal, 2002; 25(3): 1–7.

Chapman, H.D. Cation-exchange capacity. In Methods of Soil Analysis. Part 2. Chemical and Microbiological Properties, Black C.A. et al. ed. American Society of Agronomy, 1965; 9: 891-901.

Chen, Q.S., and Indraratna B. Deformation Behavior of Lignosulfonate-Treated Sandy Silt under Cyclic Loading. Journal of Geotechnical and Geoenvironmental Engineering, 01/2015; 141(1):06014015. DOI:10.1061/(ASCE) GT.1943-5606.0001210.

Chen, Q.S., Indraratna B., Carter J., and Rujikiatkamjorn C. A theoretical and experimental study on the behaviour of lignosulfonate-treated sandy silt. Computers and Geotechnics, 2014; 09/2014; 61:316–327. DOI:10.1016/j.compgeo.2014.06.010.

Chen, Q.S., and Indraratna B. Shear Behaviour of Sandy Silt treated with Lignosulfonate. Canadian Geotechnical Journal; 08/2014; DOI:10.1139/cgj-2014-0249.

Chen, Q.S., Indraratna B, Rujikiatkamjorn B. Behaviour of LS-treated Soil under Cyclic Loading. Proceedings of the Institution of Civil Engineers - Ground Improvement, 2015; 169(2):109-119.

Cullity, B.D. Elements of X-Ray Diffraction, 2nd edition, Addison-Wesley, London; 1979.

Farmer, V.C., and Russell, J.D. Interlayer complexes in layer silicates; the structure of water in lamellar ionic solutions: Transaction of Faraday Society,1971;(67): 2737-2749.

Fredheim, G.E., Braaten, S.M., and Christensen, B.E. Molecular weight determination of lignosulfonates by size-exclusion chromatography and multi-angle laser light scattering, Journal of Chromatography A, 2002; 942:191–199.

Gandini, A., and Belgacem, M. Lignin as Components of Macromolecular Materials. In Monomers, Polymers, and Composites from Renewable Resources; Eds.; Elsevier: Oxford, UK, 2008: 243–273.

Grim, R. F. Clay mineralogy. McGraw Hill, New York, 2nd edn, ch. 4 and 7, 1968.

Hang, P. and Brindley, G. Methylene blue adsorption by clay minerals; Determination of surface areas and cation exchange capacities. Clay and Clay Minerals, 1970; 18: 203-212.

Heitor, A., Indraratna, B. and Rujikiatkamjorn, C. (Laboratory study of small strain behavior of a compacted silty sand. Canadian Geotechnical Journal, 2013; 50(2): 179-188.

Indraratna, B., Muttuvel, T., Khabbaz, H., and Armstrong, R. Predicting the Erosion Rate of Chemically Treated Soil using a Process Simulated Apparatus for Internal Crack Erosion. Journal of Geotechnical and Geoenvironmental Engineering, ASCE, 2008; 134(6): 837–844.

Indraratna, B., Mahamud, M., Vinod, J.S., and Wijeyakulasuriya, V. Stabilization of an erodible soil using a chemical admixtures, In Bouassida, M, Hamdi, E & Said, I (eds), ICGE'10: Proceedings, 2nd International Conference on Geotechnical Engineering, 2010: 45-54.

Komadel, P., Madejova´, J., and Stucki, J.W. Partial stabilization of Fe(II) in reduced ferruginous smectite by Li fixation, Clays and Clay Minerals, 1999; 47: 458-465.

Petit, S., Righi, D., Madejova, J., and Decarreau, A. Interpretation of the infrared NH^{4+} spectrum of the NH^{4+}-clays; application to the evaluation of the layer charge. Clay Minerals, 1999; 34: 543-549.

Puech, P.A., Boussel, L., Belfkih, S., Lemaitre, L., Douek, P., and Beuscart, R. DicomWorks: Software for Reviewing DICOM studies and promoting low-cost releradiology, Journal of Digital Imaging, 2007; 20(2):122-130.

Ramachandran, V.S., Kacker, K.P., and Patwardhan, N.K. Adsorption of dyes by clay minerals. The American mineralogist, 1962; 47.

Rauch, A.F, Harmon, J.S., Katz, L.E., and Liljestrand, H.M. An Analysis of the Mechanisms and Efficacy of Three Liquid Chemical Soil Stabilizers, Federal Highway Administration, Report no. FHWA/TX 03/1993–1, (1), Austin, TX; 2003.

Russell, J.D., and Fraser, A.R. “Infrared methods”. In Clay Mineralogy: Spectroscopic and Chemical Determinative Methods, MJ. Wilson, ed., Chapman and Hall, London, 1996; 11-64.

Saikia, B.J., and Parthasarathy, G. “Fourier Transform Infrared Spectroscopic characterization of kaolinite from Assam and Meghalaya, Northeastern India”, Journal of Modern Physics, 2010; 1: 206-210.

Santamarina, J.C., Klein, K.A., Wang, Y.H., and Prencke, E. Specific surface: determination and relevance, Canadian Geotechnical Journal, 2002; 39:233-241.

Scholen, D. E. Non-Standard Stabilizers. Report No. FHWA-FLP-92-011, FHWA, Washington, D. C, 1992.

Scholen, D.E. Stabilizer Mechanisms in Nonstandard Stabilizers". Proceedings of 6th International Conference on Low-Volume Roads, 2, TRB, National Academy Press, Washington, D. C.,1995: 252-260.

Seed, H.B., Woodard, R.J., and Lundgren, R. Prediction of swelling potential for compacted clays. Journal of American Society of Civil Engineers, Soil Mechanics and Foundations Division, 1962; 88(3): 53– 87.

Skempton, A.W. The colloidal activity of clays. Proc. 3rd. Int. Conf. on Soil Mechanics, Vol.1, 1953; 57-61.

Taylor, J.C. Computer Programs for Standardless Quantitative Analysis of Minerals Using the Full Powder Diffraction Profile. Powder Diffraction,1991; 6: 2-9. doi:10.1017/S0885715600016778.

Tingle, J.S., Newman, J.K., Larson, S.L., Weiss, C.A., and Rushing J.F. (2007). "Stabilization mechanisms of non-traditional additives", *Transportation Research Record: Journal of the Transportation Research Board,* No. 1989, 2, Transportation Research Board of the National Academics, Washington, D.C., 2007; 59 – 67.

Theng, B.K.G. Formation and properties of clay-polymer complexes, Developments in Clay Science – Volume 4, 2nd edition, Elsevier Oxford OX5 1GB, UK, 2012.

Vinod, J.S., Indraratna, B., and Mahamud M.A.A. Stabilization of an erodible soil using a chemical admixture. Journal of Ground Improvement, 2010; 163: 43 – 51.

Whittig, L.D., and Allardice, W.R. X-ray diffraction techniques. p. 331–362 In A. Klute (ed.) Methods of soil analysis. Part 1. 2nd ed. Agron. Monogr. 9. ASA and SSSA, Madison, WI. 1986.

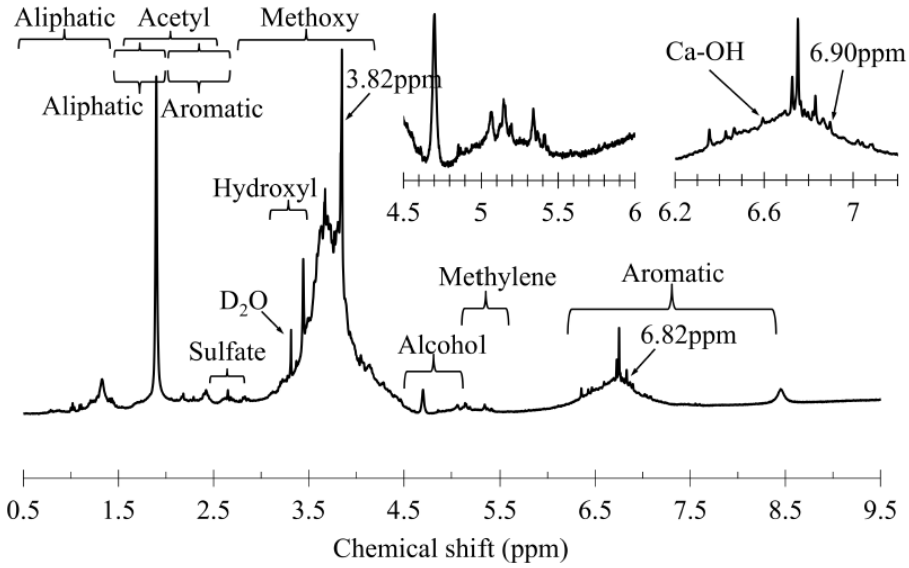

Fig. 1. H NMR spectrum of LS admixture.

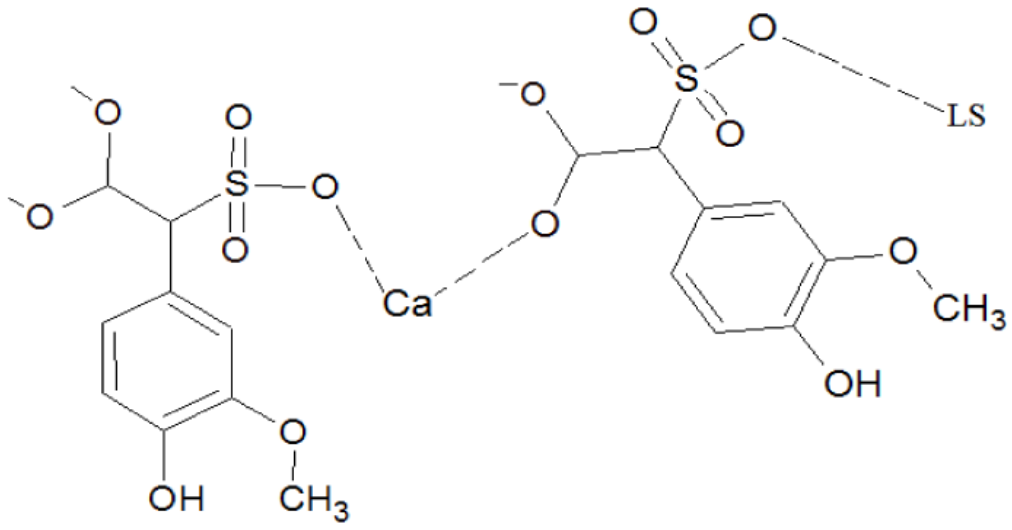

2,2-dihydroxy-1-(4-hydroxy-3-methoxyphenyl)ethanesulfonic acid

Fig. 2. Proposed chemical structure of LS admixture (after Alazigha et al. [1]).

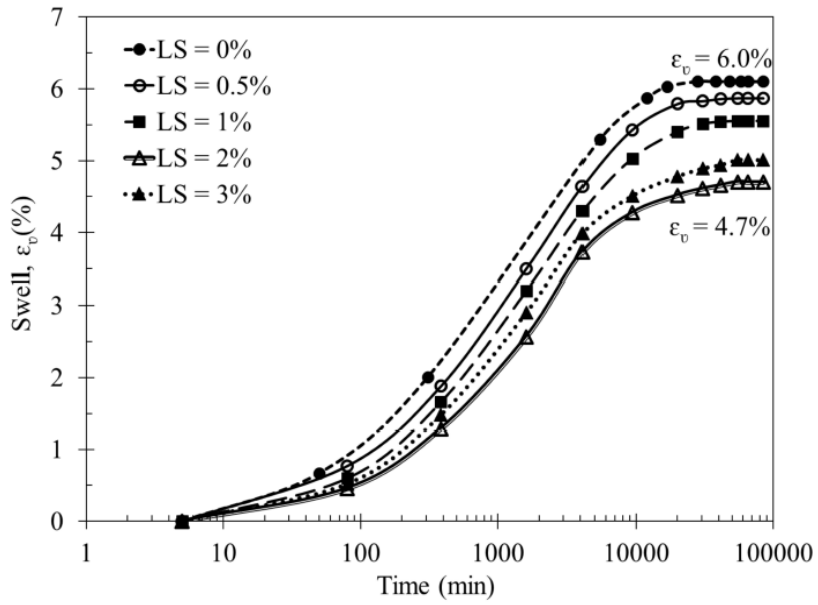

Fig. 3. Swell behaviour with time of untreated and treated expansive soil specimens.

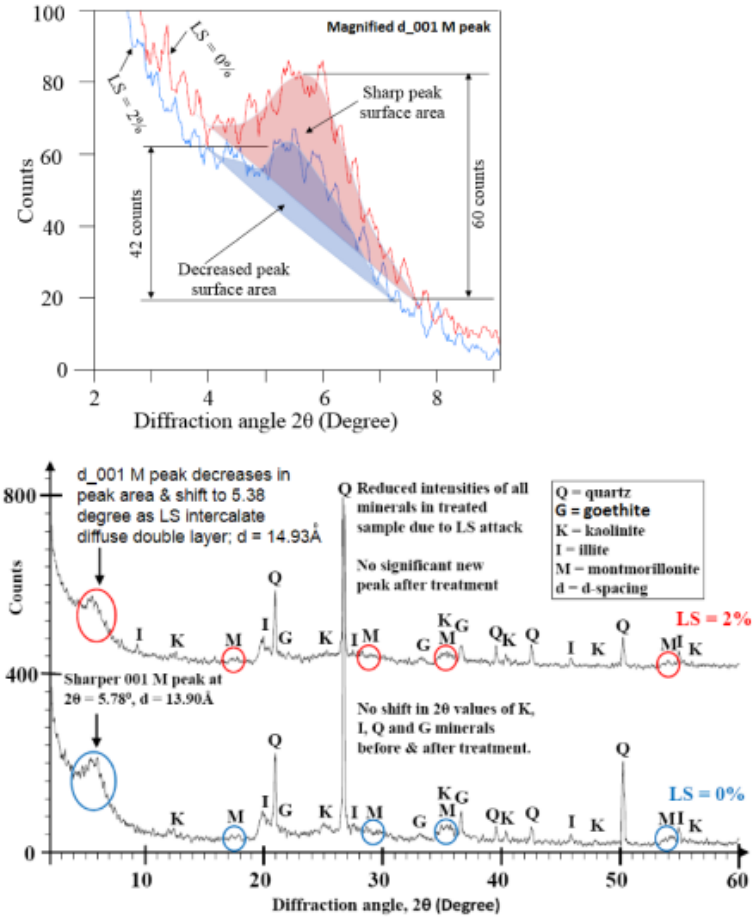

Fig. 4. XRD diffractograms of untreated (LS = 0%); and treated (LS = 2%) expansive soil.

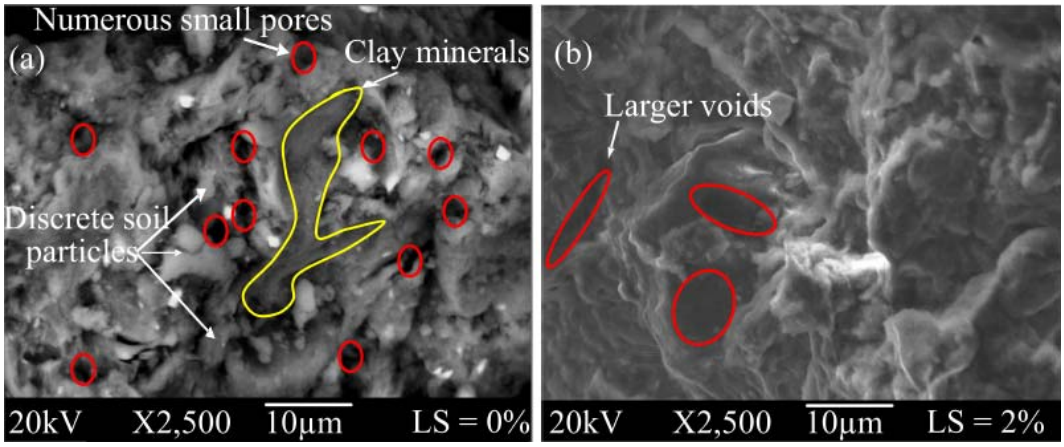

Fig. 5. SEM micrographs of (a) untreated (LS = 0%); and (b) treated (LS = 2%) expansive soil.

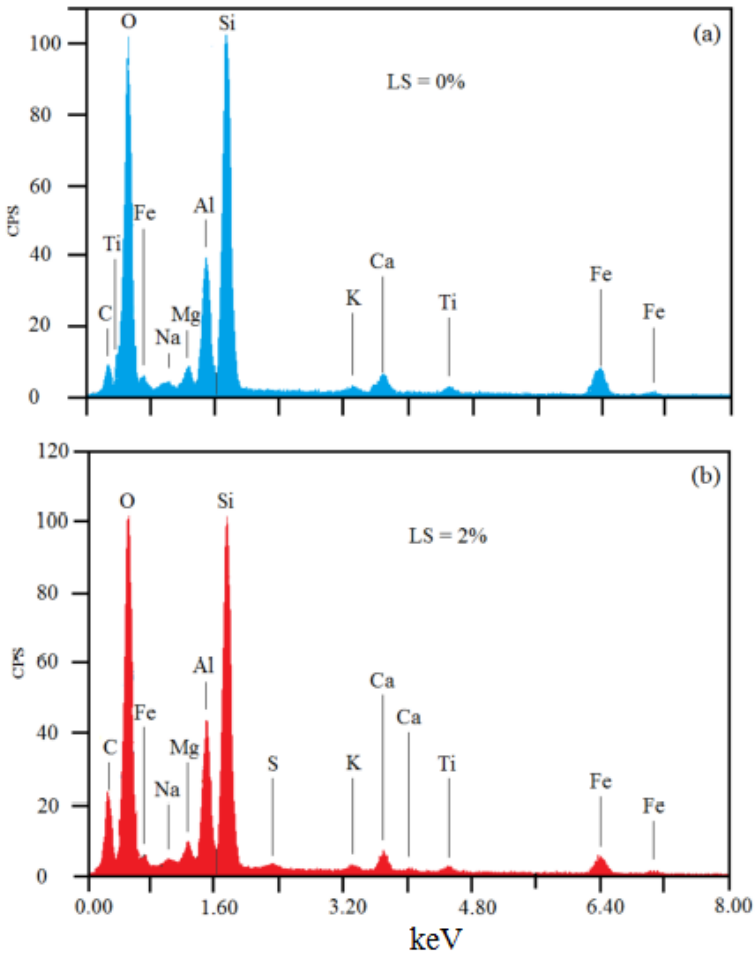

Fig. 6. EDS spectrum of (a) untreated (LS = 0%); and (b) treated (LS = 2%) expansive soil.

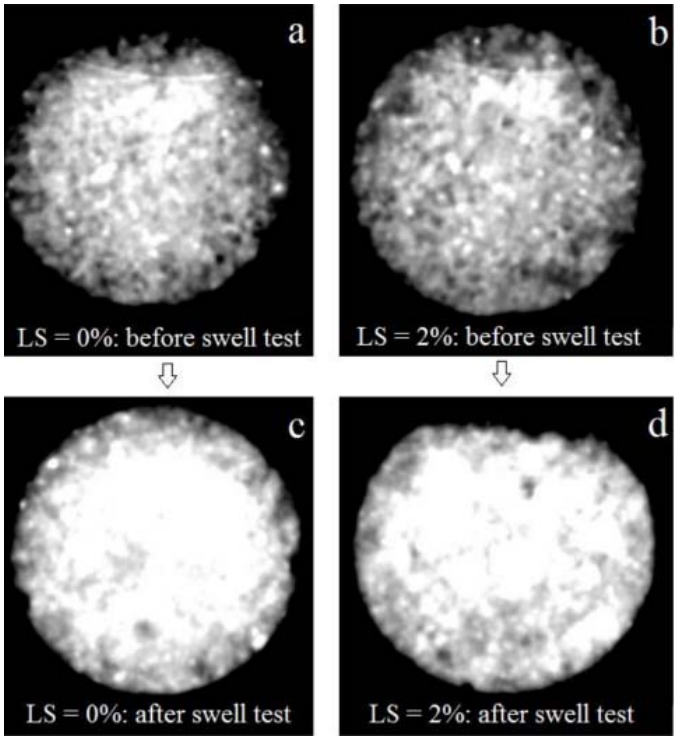

Fig. 7. CT scan images of the expansive soil specimens (a, b) before and (c, d) after swell test.

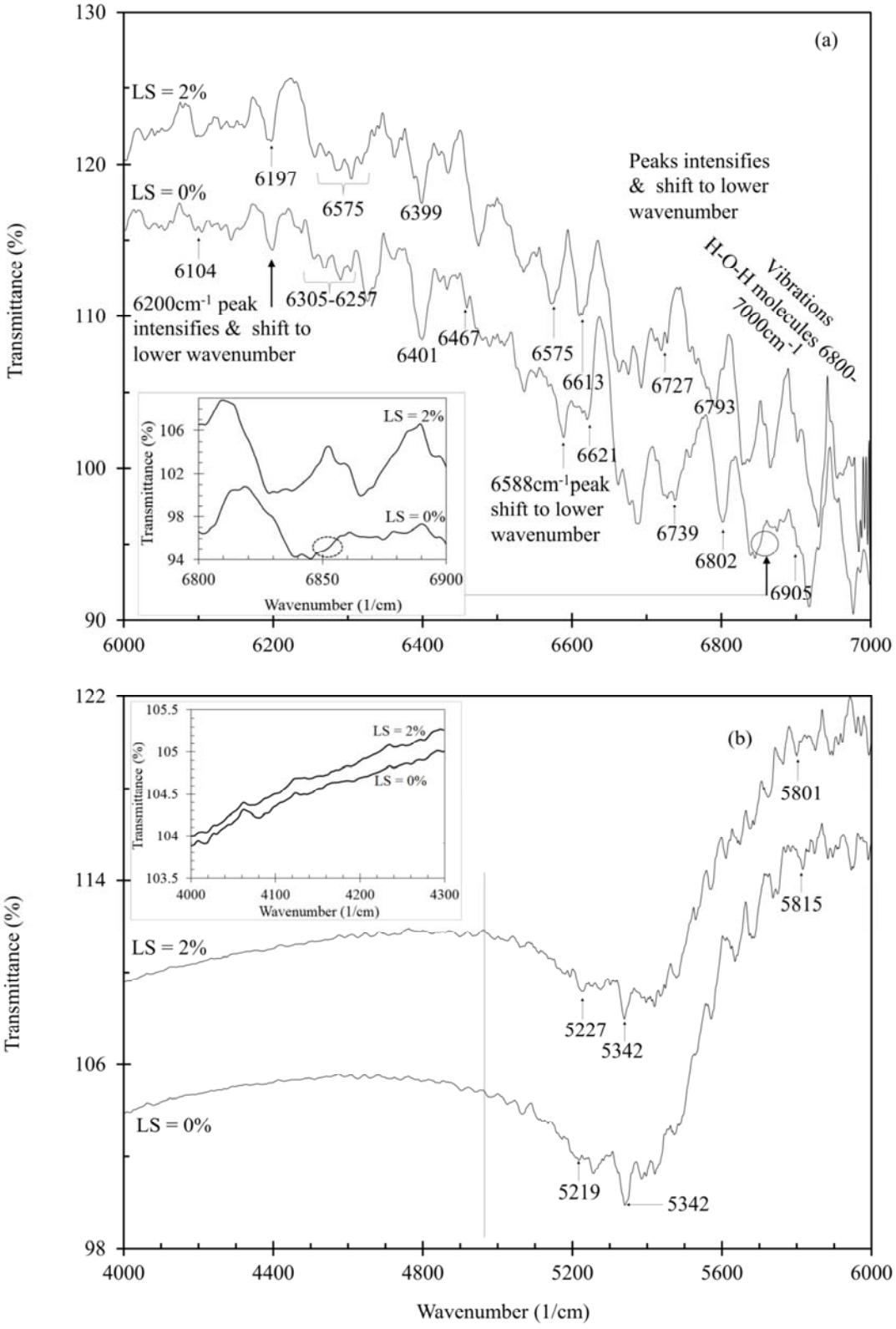

Fig. 8. FTIR patterns of untreated (LS = 0%); and treated (LS = 2%) expansive soil.

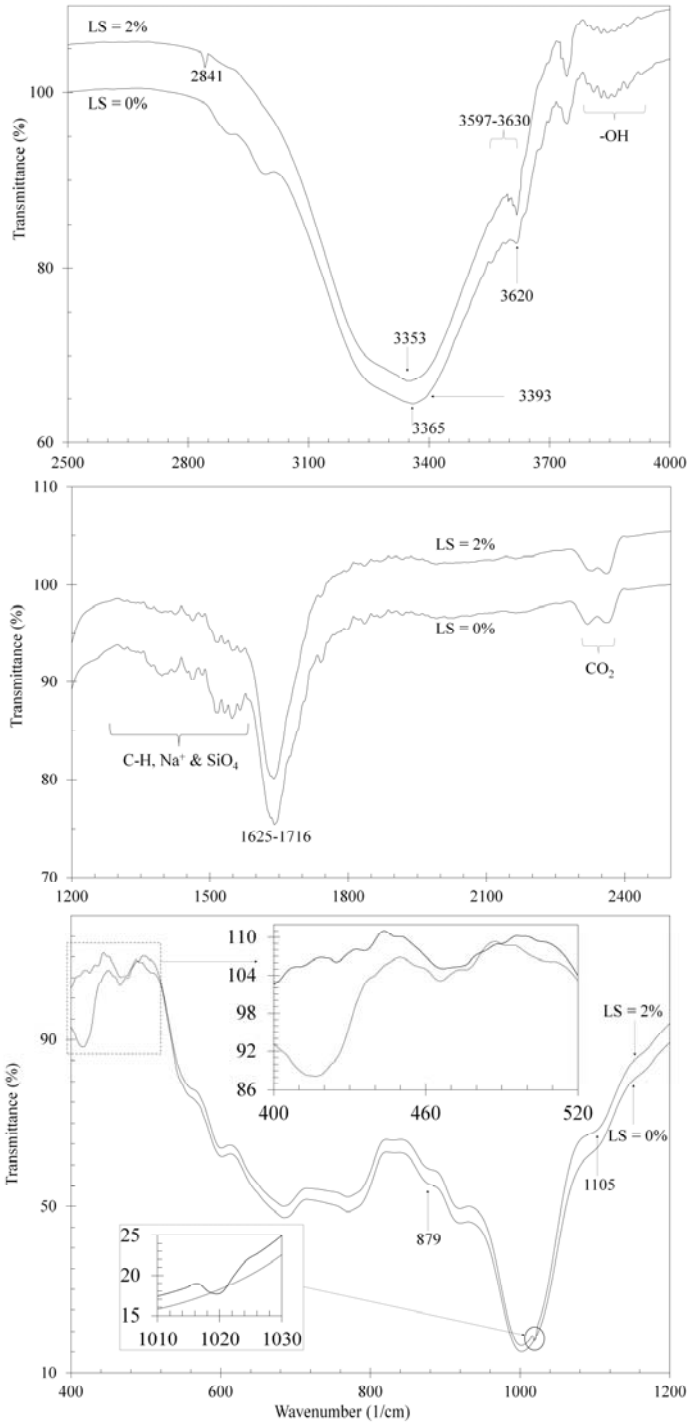

Fig. 9. FTIR patterns of untreated (LS = 0%); and treated (LS = 2%) expansive soils

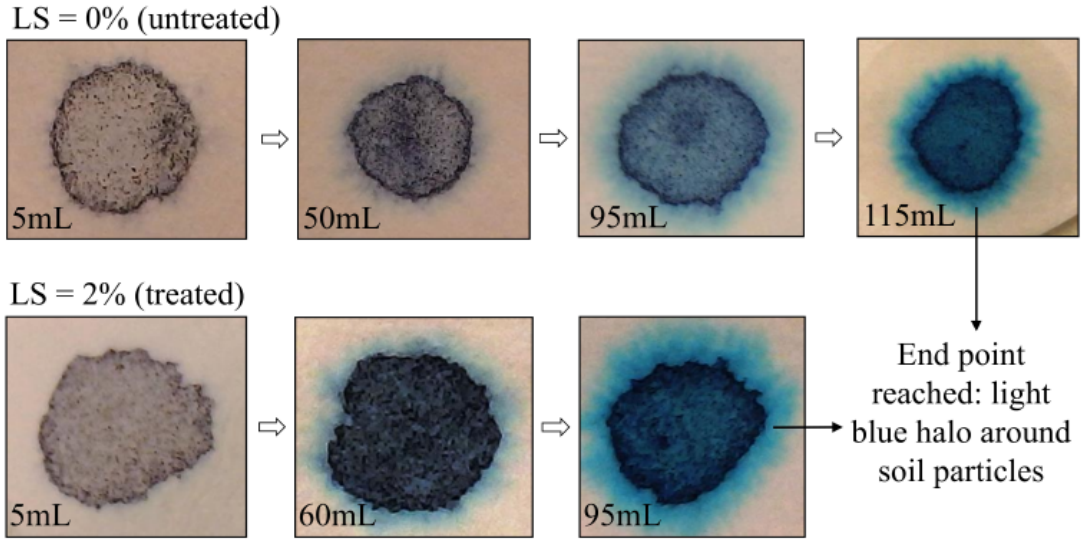

Fig. 10. Determination of CEC for untreated (LS = 0%); and treated (LS = 2%) expansive soil specimens.

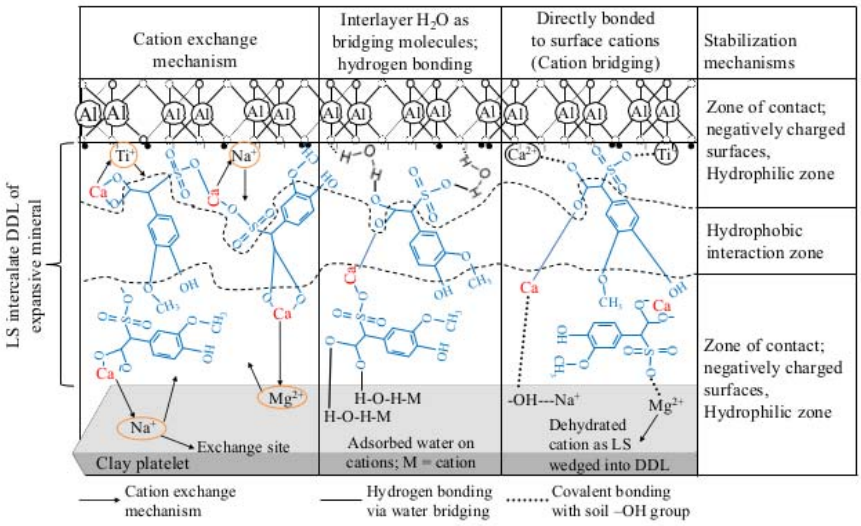

Fig. 11. Schematic illustration of the stabilization mechanisms of LS on a remoulded expansive soil.

Table 1: Physical/chemical properties of the soil (modified after; Alazigha et al., 2016)

Physical properties	**Value**	**References**
Specific gravity	2.7	AS 1289.
Natural moisture content	38	AS 1289.2.1.1-2005
Liquid limit (%)	91	AS 1289.3.9.1-2002
Plastic limit	40	AS 1289.3.2.1-2009
Plasticity index	51	AS 1289.3.9.1-2002
Shrinkage limit	9	AS 1289.7.1.1-1992
Maximum dry unit weight (MDUW), %	13.1	AS 1289.5.1.1-2003
Optimum moisture content (OMC), %	37	AS 1289.5.1.1-2003
Clay content (%)	35.6	Malvern analysis
Silt content (%)	53.8	"
Sand content (%)	8.8	"
Soil activity	1.42	Skempton (1953)
% Swell of remoulded clay at OMC and MDUW under 7kPa	6	*ASTM D4546*
Corrected swell pressure (kPa) of remoulded soil at OMC and MDUW	220	*ASTM D4546-2008*
Natural soil pH	7.43	AS 1289.4.3.1-1997
Elemental properties (EDS analysis)	**Mass (%)**	
SiO_2	55.1	EDS
Al_2O_3	19.49	"
Fe_2O3	13.33	"
CaO	2.69	"
MgO	3.56	"
TiO_2	0.16	"
Na_2O	0.21	"
LOI	5.45	"
Cation exchange capacity (CEC)	57.5meq/100g	ASTM C837-2014
Specific surface area (SSA) of soil	61.75m^2/g	ASTM C837-2014

NOTE: The corrected swell pressure of the remoulded soil was determined using the procedure described by Fredlund (1983).

Table 2: Interpretation of FTIR bands of the Lignosulfonate admixture

S/No.	Band position (cm-1)	Origin	Assignments
1	1041	C-O-C	Stretching vibration
2	1220	C-O	Phenol stretching
3	1221	C-C, C-O	Stretching vibration
4	1190	S-O	Sulfonic group
5	1334	O-H	Binding vibration
6	1423	C-C, C-H	Aromatic skeleton, C-H in-plane deformation
7	1460	C-H	Deformation (asymmetric in methyl and methylene group
10	1553	Ca^{2+}	Calcium-bound state
11	1508, 15517, 1594	C=C	Aromatic skeletal vibration
12	1600	C-H	Vibration of aromatic ring
13	2845	$O\text{-}CH^{3}$	stretching (methoxyl group)
14	2930	C-H	stretching (methyl and methylene group)
15	3396	O-H	Hydroxy group, H-bonded OH stretch (phenolic and aliphatic hydroxyl group)